

PHYSICAL REVIEW B

CONDENSED MATTER

THIRD SERIES, VOLUME 47, NUMBER 23

15 JUNE 1993-I

Spin polarization of core-level photoelectrons

T. Kachel* and C. Carbone

Institut für Festkörperforschung, Forschungszentrum Jülich, D-5170 Jülich, Germany

W. Gudat

Berlin Elektronenspeicherringgesellschaft für Synchrotronstrahlung m.b.H., BESSY, D-1000 Berlin 33, Germany

(Received 22 January 1993)

Spin-resolved core-level photoemission spectra of the ferromagnetic transition metals have been measured with synchrotron radiation. The experimental results show in all cases a pronounced dependence of the core-electron spectral distribution on the spin orientation of the photoemitted electrons. The results are compared with a simple model, based on the exchange splitting of atomic multiplets, which takes into account the spin coupling between the photoelectron and the photoionized atom. An interpretation is proposed that relates the spin polarization of the main spectral features to the final-state local spin momentum.

I. INTRODUCTION

X-ray photoemission studies^{1,2} on solids have shown that the excitation of core electrons into continuum states produces complex spectral distributions when outer subshells of the emitting atoms contain localized electrons with unpaired spins. Core-level photoemission spectra can be significantly influenced by the final-state spin and orbital momentum coupling of the core hole to the incomplete valence subshells.^{1,2}

The study of the core-electron photoemission spectra of magnetic $3d$ materials has attracted much attention.³ The detailed understanding of spin-dependent effects in the core-level photoexcitation has wide implications in several fields such as, for example, spin-dependent x-ray absorption, magnetic circular dichroism, and spin-polarized photoelectron diffraction. Furthermore, much of the experimental activity was based on an attempt to use the spectroscopy of core levels as a quantitative probe of localized ground-state magnetic moments.⁴⁻⁸ However, a simple correlation between the spectral features and the localized magnetic moments has so far not emerged from experimental works.⁸

The available quantitative theories of inner-shell photoexcitation including spin-dependent interactions are limited in their applicability to real systems, since they are largely based on atomic models.⁹ The atomic final-state multiplet theory accounts well for the spectra of ionic $3d$ compounds⁹ but its application has been ques-

tioned whenever the $3d$ states have significant itinerant character.¹⁰ Electron hopping, hybridization, and interatomic relaxation have been included in model calculations by Kakehashi *et al.*^{10,11} The importance of these effects in determining the energetics, the line shape, and, in particular, the spin polarization of core-level spectra still needs to be established experimentally. This is a necessary condition for retrieving reliable information on the ground-state configuration from core-level spectroscopy. The direct measure of the photoelectron-spin polarization should be able to help in clarifying these issues. However, the available spin-resolved core-level data are still scarce.¹²⁻¹⁶

The Fe $3s$ spectra are considered a good test case since they are not complicated by core-hole spin-orbit coupling. Recently, we have demonstrated that the intra-atomic exchange interaction is the main cause for the splitting of the $3s$ emission¹³ in accord with previous interpretations. Hillebrecht, Jungblut, and Kisker¹⁶ studied the same subject and arrived at the conclusion that it cannot be explained by the current theoretical models.

In this paper we present additional evidence that the core-level photoemission spectral distributions of all pure transition-metal ferromagnets depend on the spin of the emitted electrons. Following our experiments on the Fe $3s$, we have studied the spin-resolved spectral distributions of the $3p$ subshell. We shall discuss these results together with those of the Fe $3s$ emission.^{13,14} We examine the applicability and the limits of a simple theoretical

model for the interpretation of the spin polarization in core-level spectra, which takes into account the spin coupling between the photoelectron and the photoionized atom. A qualitative interpretation is proposed for the spin polarization of the main spectral features, which relates the spin polarizations to their final-state spin momentum.

II. EXPERIMENTAL DETAILS

The measurements were performed on the TGM5 undulator-wiggler beam line¹⁷ at BESSY. Fe(100) and Ni(100) single crystals were prepared *in situ* by repeated sputtering and annealing cycles, monitored by Auger spectroscopy and low-energy electron diffraction (LEED). Thick (≥ 100 Å) Co films were deposited *in situ* on the Fe single crystal. The samples, shaped as picture frames, were magnetically saturated by applying a pulsed current to a coil wrapped around one of the legs of the crystal and measured in the remanent state at room temperature. Monochromatic, *s*-polarized synchrotron radiation was used for electron excitation. Energy distribution curves were measured at normal emission with a 90° spherical electron analyzer at a total resolution of about 500 meV. The spin analysis was performed by high-energy Mott scattering. As usual, we define as spin-up (spin-down) electrons those with spin momentum parallel (antiparallel) to the macroscopic magnetization direction. The degree of spin polarization P is defined as $P = (N^\uparrow - N^\downarrow) / (N^\uparrow + N^\downarrow)$, where N^\uparrow and N^\downarrow are the numbers of the spin-up and spin-down electrons, respectively.

III. THEORETICAL MODEL

We examine, in the following, how the main features and their spin polarizations can be compared to the expectations of a theoretical picture based on final-state multiplet splitting. In particular, we discuss the relation between the spin multiplicity of a final state and the total spin polarization. We follow the approach of Alvarado and Bagus,¹⁸ who discussed the photoemission from localized atomic 3*d* shells in ferromagnetically ordered systems (at $T = 0$ K). This model has been extended to core-level emission in calculations by Rothberg¹⁹ and by Sinkovic, Friedman, and Fadley²⁰ along the same line. The main assumption is that the initial-state total spin S^i and its projection along the quantization (magnetization) axis S_z^i are conserved in the total system (ion plus photoelectron) upon photoionization. Thus, the conservation of the total spin momentum implies that the ionic state reached after photoionization can be either a low-spin final state with $S^f = S^i - \frac{1}{2}$ or a high-spin final state with $S^f = S^i + \frac{1}{2}$. The conservation of S_z^i implies that the projection of the electron-spin momentum s_z enters by the equation $S_z^i = S_z^f + s_z$. For the low-spin final state this requires that the photoelectron must have spin $s_z = +\frac{1}{2}$ (spin up, $P = +100\%$). The final-state wave function of the system for the low-spin state can be written as the product of the ion and the continuum electron states:

$$\Psi(S, S_z) = A |S - \frac{1}{2}, S - \frac{1}{2}\rangle | \frac{1}{2}, \frac{1}{2}\rangle .$$

In the high-spin final state the photoelectron can have either $s_z = -\frac{1}{2}$ (spin down) or $s_z = +\frac{1}{2}$ (spin up), depending on whether $S_z^f = S^f = S_z^i + \frac{1}{2}$ or $S_z^f = S^f - 1 = S_z^i - \frac{1}{2}$. The final-state wave function for the high-spin final state is thus

$$\Psi(S, S_z) = B |S + \frac{1}{2}, S + \frac{1}{2}\rangle | \frac{1}{2}, -\frac{1}{2}\rangle + C |S + \frac{1}{2}, S - \frac{1}{2}\rangle | \frac{1}{2}, \frac{1}{2}\rangle .$$

The coefficients A , B , and C can be calculated as in Ref. 17, resulting in a calculated photoelectron-spin polarization for the high-spin final states:

$$P = -\frac{B - C}{B + C} = -\frac{2S^f - 1}{2S^f + 1} .$$

The relation of P to S^f is shown in Fig. 1. As a direct consequence the high-spin and low-spin final states, which are expected to be separated in energy by the exchange interaction, can also be distinguished by the photoelectron-spin polarization. We summarize the predictions of the model as follows: (1) The photoemitted electrons in transitions leading to a low-spin final state should be fully spin-up polarized; (2) those transitions corresponding to a high-spin final state result in mostly spin-down emission, but they should *not* be fully polarized. We show that the simple correlation discussed above between spin polarization and final-state spin momentum can account, at least qualitatively, for the experimental results of the Fe 3*s* emission and the emission of 3*p* electrons of Fe, Co, and Ni, to be discussed in detail in the following. Finally, we emphasize that our experimental and theoretical results concerning the spin-resolved Fe 3*s* spectrum compare well to very recent cal-

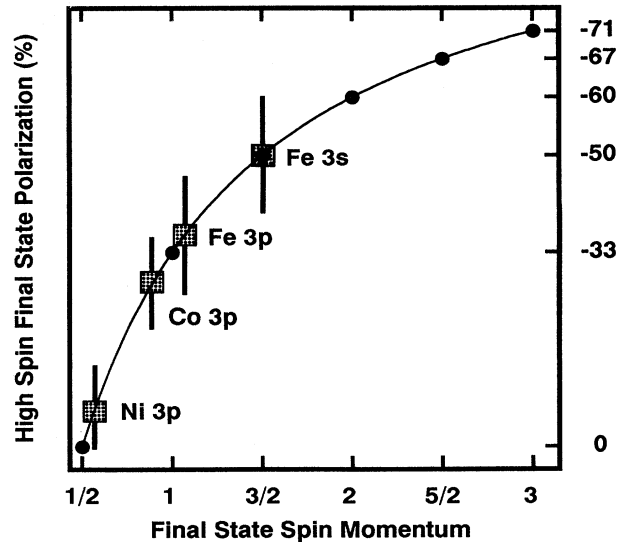


FIG. 1. Correlation between the spin polarization of high-spin final states and final-state spin momenta (solid line). The full dots represent half-integer momenta. Measured polarization values for Fe, Co, and Ni 3*p* and Fe 3*s* are indicated. Note that the polarization is negative.

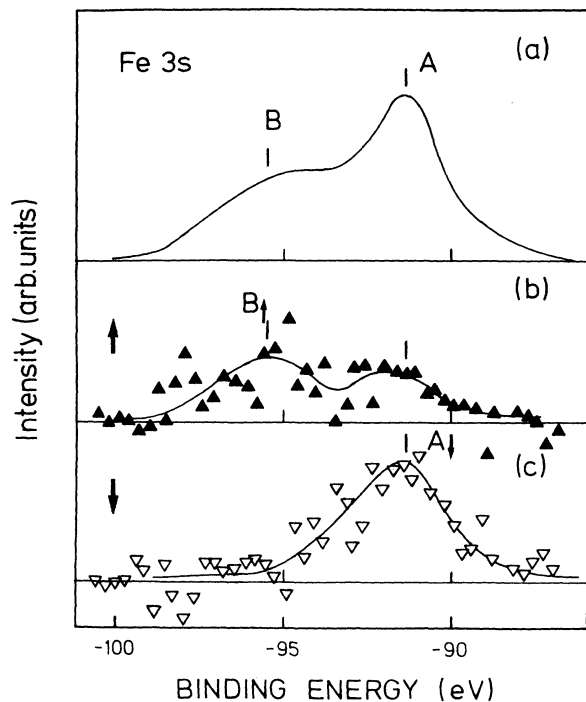


FIG. 2. Spin-resolved background-subtracted Fe 3s spectrum. (a) Spin integrated, (b) spin up, (c) spin down. Peaks *A* and *B* denote high- and low-spin peaks, respectively. The figure is adapted from Ref. 14.

culations by Thole and van der Laan.²¹ They outlined a group-theory-based determination of spin polarizations and magnetic dichroism in photoemission.

IV. RESULTS AND DISCUSSION

A. The Fe 3s spectrum

In Fig. 2 we reproduce the background-subtracted spin-resolved and spin-integrated Fe 3s spectra from our previous work.¹⁴ All the relevant features, intensity, line shape, and binding energy are in good agreement with the data of Hillebrecht, Jungblut, and Kisker.¹⁶ Thus,

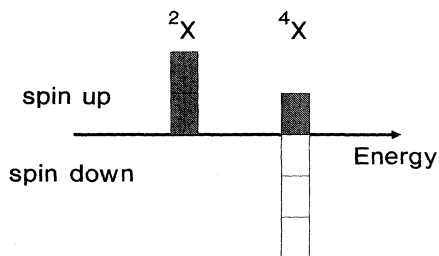


FIG. 3. Spin-dependent energy-level diagram for nondegenerate (exchange split) doublet and quartet states representing the Fe 3s final states. 2X and 4X final states were chosen to model the average Fe-metal ground-state magnetic moment of $2.3\mu_B$ ($\approx 2\mu_B \rightarrow ^3X$ initial state).

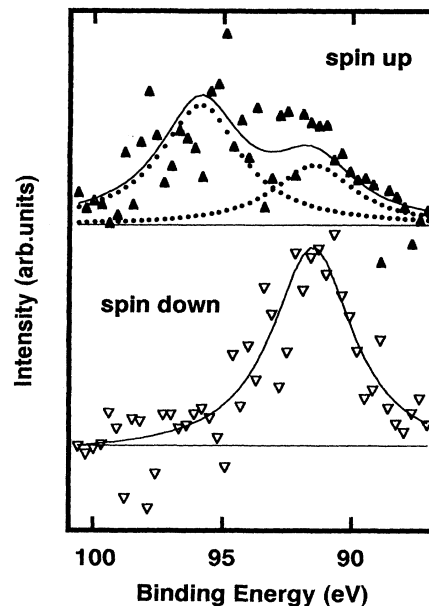


FIG. 4. The Fe 3s spectrum: comparison of the model (Fig. 3) to the experimental data. Triangles: measured data after background subtraction; solid lines: theoretical results representing the broadened level diagram in Fig. 3; dotted lines: high- and low-spin components of the spin-up emission.

our conclusions hold for their data as well. The experimental results show that the two features in the spin-resolved spectra correspond to structures in the two opposite spin channels, mostly spin-up emission for the low-spin and mostly spin-down emission for the high-spin final state. The spin-up emission extends over nearly 10 eV as already pointed out in Refs. 14 and 16. The total spin-up to spin-down intensity ratio is measured to be 1.1.¹⁶ On the basis of the atomic model one expects a $3s^13d^8$ final state giving rise to a doublet low-spin and a quartet high-spin final state, separated in energy due to the exchange interaction. In the atomic picture their intensity is proportional to the spin multiplicity of the final states, so one arrives at the spin distribution given in Fig. 3. Folding the schematic spin distribution results in a spin-resolved spectral distribution as shown in Fig. 4. The direct comparison to the experimental data demonstrates the applicability of the atomic model in contrast to the statements by Hillebrecht, Jungblut, and Kisker.¹⁶ Since both high-spin and low-spin final states separated by 4.4 ± 0.3 eV contribute to the spin-up Fe 3s emission this simply explains why the spin-up spectrum has a linewidth of 10 eV. The total, energy-integrated spin-up to spin-down emission density ratio is expected to be equal to 1, obviously in close agreement with the experimental observations. Small deviations might arise from configuration interaction effects.

B. Fe, Co, and Ni 3p spectra

In Figs. 5–7 we present spin-resolved and spin-summed energy distribution curves of the Fe, Co, and Ni 3p levels. The *p* emission appears in both spin channels

superimposed to the polarized background of inelastically scattered electrons. The polarization of the inelastic secondary-electron backgrounds is 28% in Fe, 20% in Co, and 6% in Ni, as is indicated by the offset between the spin-resolved curves. In the Fe 3*p* and Co 3*p* spectra a single peak is found in each spin channel. The 3*p* peaks in the opposite spin channels differ in intensity, line shape, and binding energy. The Fe 3*p* spin-up peak is shifted by 0.45 ± 0.1 eV to higher binding energy than the spin-down peak, in agreement with Ref. 14. The Co 3*p*

spin-up structure is at 0.15 eV higher binding energy than the spin-down one. The Fe 3*p* spin-up peak has a full width at half maximum of 2.6 ± 0.2 eV, whereas the spin-down peak is only 1.7 ± 0.2 eV wide. For Co the widths of the spin-up and the spin-down peaks is 2.4 ± 0.2 eV. The effective spin polarization, P_{eff} , calculated by energy integrating over the 3*p* peaks after subtraction of the background indicated in Fig. 5(c), is found to be -35% in Fe and -27% in Co.

The spin-resolved spectra for the Ni 3*p* levels (Fig. 7) show spin-down emission at lower binding energy than the spin-up one in the main peak region *A*. The asymmetric line shape of these structures suggests the pres-

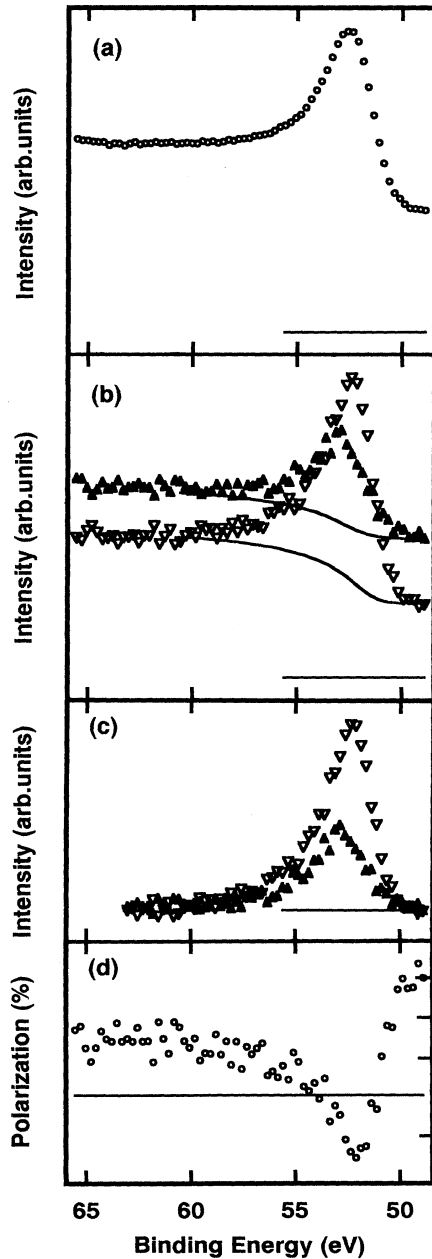


FIG. 5. Fe 3*p* spectrum: (a) spin integrated; (b) spin resolved as measured (Δ , spin up; ∇ , spin down), the solid lines giving an example of the background subtraction applied; (c) spin resolved after background subtraction; (d) spin polarization.

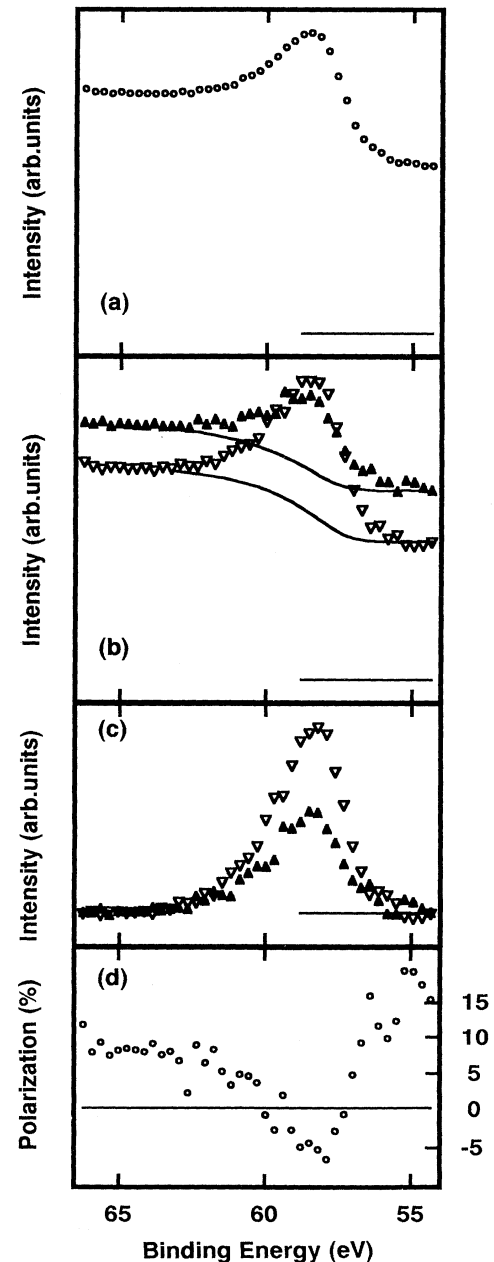


FIG. 6. Co 3*p* spectrum analogous to Fig. 5.

ence of overlapping unresolved contributions. The polarization of the Ni 3*p* main peak is -5% . In the “6-eV satellite” region *B*, weak spin-up and spin-down structures are found at different energies.

The results presented in Figs. 5–7 demonstrate that the contribution of the 3*p* levels from these ferromagnetic metals is strongly spin dependent, regarding the core-level intensity, binding energy, and line shape. All the spectra show mostly spin-down emission at low binding energy, an expected consequence of the core-valence exchange interaction.

We first discuss the experimental data on the Fe and Co 3*p* polarization within the theoretical frame presented above. On the basis of a Hartree-Fock calculation of the $3p^5 3d^8$ final state the Fe 3*p* emission should be spread over a large energy region. Our data do not give evidence of high binding-energy features corresponding to low-spin final states, indicating that the transition probabilities to these final states are small. Rather, we observe the

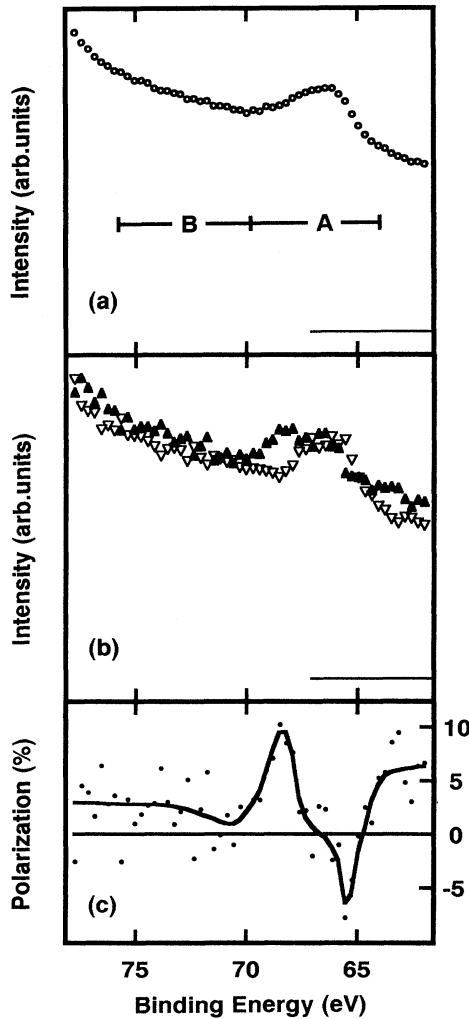


FIG. 7. Ni 3*p* spectrum analogous to Figs. 5 and 6 but missing the background-subtracted curves. Regions *A* and *B* separate the “main peak” and the “satellite” regions, respectively.

two high binding-energy features described above. We attribute these peaks, as in Ref. 5, to the excitation of the lower energy and high-spin multiplet terms only. The sign and the magnitude of their spin polarization support this identification. The polarization of the main 3*p* spectral features can be compared to the calculated values equal to $(2S_f - 1)/(2S_f + 1)$, expected for the high-spin final states. The measured values of the spin polarizations of the Fe 3*s* and the Fe, Co, and Ni 3*p* emission are plotted in Fig. 1. The spin polarization of the Fe 3*p* peak of -35% , is similar to the Fe 3*s* high-spin final-state polarization. The Co 3*p* peak polarization, about -27% , corresponds approximately to a triplet final state. The Ni main peak polarization is about -5% , as expected for a high-spin final-state momentum with $\frac{1}{2} \leq S \leq 1$. The experimental data show qualitatively the expected trend, with the spin polarizations of the high-spin final states decreasing along the 3*d* series with increasing *d* occupancy, that is, with decreasing spin momentum in the final states. The value of the polarizations decreases going from Fe to Co and to Ni, as expected for incremental increase of the *d* occupancy by one unit. In all cases the sign of the spin polarizations of the high-spin final states is negative as expected.

In the following we discuss the line shape of the Fe, Co, and Ni 3*p* emission. We suggest that a small energy splitting (0.4 eV in Fe and 0.15 eV in Co) between spin-up and spin-down 3*p* peaks can be attributed, within the atomic model, to the lifting of the degeneracy between the two high-spin final-state configurations with equal S^f and different S_z^f (i.e., S_z^f vs $S_z^f - 1$) when the ion is immersed in a ferromagnetic system.

The Ni spectra presented in Fig. 7 can be discussed along a similar line. We consider the $3p^5 3d^{10}$ final-state configuration corresponding to the emission in the main peak region *A* in the figure. In Ni the 3*p* spin-orbit interaction cannot be neglected in comparison to the exchange. If the single-hole final state can be described in a mean magnetic-field approximation, the degeneracy between the single-hole final states, which belong to the same *J* value, is removed according to the M_J eigenvalues. Thus, the $J = \frac{3}{2}$ and $\frac{1}{2}$ spin-orbit split peaks, which are spin independent as single entities, break down into a set of spin-polarized multiplets. These states can be writ-

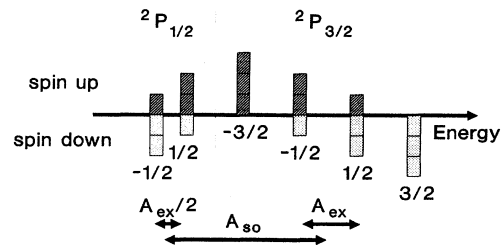


FIG. 8. Spin-dependent energy-level diagram for nondegenerate $^2P_{3/2}$ and $^2P_{1/2}$ states representing the Ni $3p^5 3d^{10}$ final states. The spin-orbit splitting and the exchange splitting, which are different for the $P_{3/2}$ and the $P_{1/2}$ states, as well as the M_J quantum numbers are indicated.

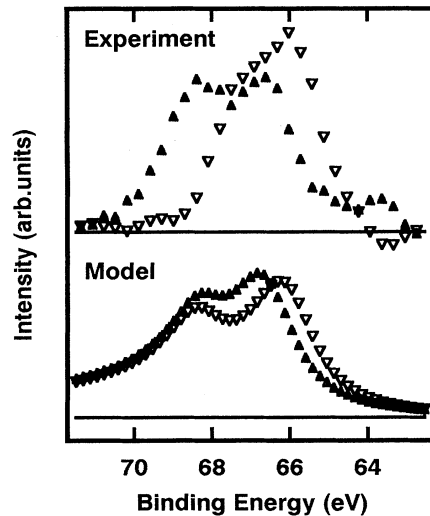


FIG. 9. The Ni 3p spectrum: comparison of the model (broadened final states of Fig. 8 to the background-subtracted experimental data). Δ , spin up; ∇ , spin down.

ten as a combination of spin and orbital momentum wave functions in the limit of a weak magnetic field and a large spin-orbit interaction. The results are shown schematically in Fig. 8 and are compared to the main Ni 3p peak (Fig. 9), which is attributed essentially to the $3p^5 3d^{10}$ configuration. Although it was not our aim to optimize the details of the curve fitting, in view of the crudeness of the model, we could determine the splitting between the

pure spin-up and spin-down states to be constrained between 0.3 and 0.9 eV. This value compares favorably with the calculated Ni 3p spin-up and spin-down energy splitting (0.68 eV) predicted by local-spin-density theory.²²

As a final remark we point out that, within the simple picture described in Sec. III and compared here to the experimental results, only the final-state spin multiplicity of a given term is directly related to its spin polarization. The measured spin polarization of the high-spin terms could be used to determine the final-state spin momentum. However, the screening of the core hole in the solid certainly needs to be taken into account in this picture. Thus the experimental values of the spin polarizations have to be seen as reflecting the (screened) final-state local spin configuration rather than the ground-state moment. We suggest that the measurement of the polarization of the high-spin multiplet term emission from core levels might provide a more direct guide to the final local moment than the 3s energy splitting.

V. CONCLUSIONS

Spin-dependent spectral distributions of core levels have been experimentally determined by spin-resolved photoemission. Core-level intensities, line shapes, and binding energies depend on the photoelectron spin. The results are compared to the theoretical expectations on the basis of a final-state atomic multiplet picture. This model provides a simple interpretation for the spin polarization of the main spectral features, including those of the Fe 3s.

*Present address: BESSY, D-1000 Berlin, Germany.

- ¹C. S. Fadley, D. A. Shirley, A. J. Freeman, P. S. Bagus, and J. V. Mallow, *Phys. Rev. Lett.* **23**, 1397 (1969).
- ²C. S. Fadley and D. A. Shirley, *Phys. Rev. A* **2**, 1109 (1970).
- ³D. A. Shirley, in *Photoemission in Solids*, edited by M. Cardona and L. Ley (Springer, Berlin, 1978), Vol. 1, p. 165.
- ⁴F. M. McFeely, S. P. Kowalczyk, L. Ley, and D. A. Shirley, *Solid State Commun.* **15**, 1051 (1974).
- ⁵J. Ayouley and L. Ley, *Solid State Commun.* **31**, 131 (1979).
- ⁶C. Binns, C. Norris, G. P. Williams, M. G. Barthes, and H. Padmore, *Phys. Rev. B* **34**, 8221 (1986).
- ⁷H. I. Starnberg, M. T. Johnson, D. Pescia, and H. P. Hughes, *Surf. Sci.* **178**, 336 (1986).
- ⁸J. F. van Acker, Y. M. Stadnik, J. C. Fuggle, H. J. W. Hoekstra, K. H. J. Buschow, and G. Stronik, *Phys. Rev. B* **37**, 6827 (1985).
- ⁹P. S. Bagus, A. J. Freeman, and F. Sasaki, *Phys. Rev. Lett.* **30**, 850 (1973); A. J. Freeman, P. S. Bagus, and J. V. Mallow, *Int. J. Magn.* **4**, 35 (1973).
- ¹⁰Y. Kakehashi, K. Becker, and P. Fulde, *Phys. Rev. B* **29**, 16 (1984); Y. Kakehashi, *ibid.* **32**, 1607 (1985).
- ¹¹Y. Kakehashi and A. Kotani, *Phys. Rev. B* **29**, 4292 (1984).

- ¹²C. Carbone and E. Kisker, *Solid State Commun.* **65**, 1107 (1988).
- ¹³C. Carbone, T. Kachel, R. Rochow, and W. Gudat, *Z. Phys. B* **79**, 325 (1990).
- ¹⁴C. Carbone, T. Kachel, R. Rochow, and W. Gudat, *Solid State Commun.* **77**, 619 (1991).
- ¹⁵B. Sinkovic, P. D. Johnson, and N. B. Brookes, *Phys. Rev. Lett.* **65**, 1647 (1990).
- ¹⁶F. U. Hillebrecht, R. Jungblut, and E. Kisker, *Phys. Rev. Lett.* **65**, 2450 (1990).
- ¹⁷W. Peatman, C. Carbone, W. Gudat, W. Heinen, P. Kuske, J. Pflüger, F. Schäfers, and T. Schröter, *Nucl. Instrum. Methods, Phys. Res.* **60**, 1445 (1989).
- ¹⁸S. F. Alvarado and P. S. Bagus, *Phys. Lett.* **67A**, 397 (1978).
- ¹⁹G. M. Rothberg, *J. Magn. Mater.* **15-18**, 323 (1980).
- ²⁰B. Sinkovic, D. J. Friedman, and C. S. Fadley, *J. Magn. Mater.* **92**, 301 (1991).
- ²¹B. T. Thole and G. van der Laan, *Phys. Rev. B* **44**, 12424 (1991).
- ²²E. Wimmer, A. J. Freeman, and H. Krakauer, *Phys. Rev. B* **30**, 3113 (1984).